# Mobilization of Selenite by *Ralstonia metallidurans* CH34

MURIELLE ROUX,[1] GÉRALDINE SARRET,[2] ISABELLE PIGNOT-PAINTRAND,[3] MARC FONTECAVE,[1]
AND JACQUES COVES[1]*

*Laboratoire de Chimie et Biochimie des Centres Redox Biologiques, CEA-Grenoble, DBMS/CB-CNRS-Université
Joseph Fourier,[1] and Atelier de Microscopie Electronique, IFR 27 INSERM, CEA-Grenoble,[3] 38054 Grenoble Cedex 9,
and Laboratoire de Géophysique Interne et Tectonophysique, Université Joseph Fourier,
38041 Grenoble Cedex,[2] France*

**Ralstonia metallidurans CH34 (formerly *Alcaligenes eutrophus* CH34) is a soil bacterium characteristic of metal-contaminated biotopes, as it is able to grow in the presence of a variety of heavy metals. *R. metallidurans* CH34 is reported now to resist up to 6 mM selenite and to reduce selenite to elemental red selenium as shown by extended X-ray absorption fine-structure analysis. Growth kinetics analysis suggests an adaptation of the cells to the selenite stress during the lag-phase period. Depending on the culture conditions, the medium can be completely depleted of selenite. Selenium accumulates essentially in the cytoplasm as judged from electron microscopy and energy-dispersive X-ray analysis. Elemental selenium, highly insoluble, represents a nontoxic storage form for the bacterium. The ability of *R. metallidurans* CH34 to reduce large amounts of selenite may be of interest for bioremediation processes targeting selenite-polluted sites.**

In aerated environments, selenium can exist in several redox forms, including the elemental form, Se(0), which is a solid, and the oxidized forms, selenite ($SeO_3^{2-}$) and selenate ($SeO_4^{2-}$), which are bioavailable, mobile, and toxic for many organisms (5). Selenium is widely distributed in virtually all materials of the earth's crust, but accumulation of toxic compounds of selenium can also have an anthropogenic source. Selenium and its derivatives are widely used in industrial products, and the problem of selenium accumulation remains in mind after the ecological disaster of Kesterson National Wildlife Refuge, in California, due to agricultural drainage released in the Kesterson Reservoir (19). Since microorganisms are involved in the geochemical cycle of selenium, soil bacteria may thus be used in bioremediation processes. Some of them are able to resist high concentrations of a variety of metals and oxyanions (16), and the reduction of selenite to selenium by the common aerobic soil bacterium *Bacillus subtilis* (10) or the phototrophic purple nonsulfur bacterium *Rhodospirillum rubrum* (12) has been reported. The accumulation of selenium by *Rhodobacter sphaeroides* has been also reported very recently (23).

*Ralstonia metallidurans* CH34 (formerly *Alcaligenes eutrophus* CH34) is a microorganism characteristic of metal-contaminated biotopes (14). It has been previously demonstrated to have detoxification pathways for a broad range of metals, as it bears two megaplasmids controlling resistance against $Cd^{2+}$, $Co^{2+}$, $Zn^{2+}$, $Tl^{2+}$, $Cu^{2+}$, $Pb^{2+}$, $Ni^{2+}$, $Hg^{2+}$, and $CrO_4^{2-}$. Resistance is due mainly to plasmid-mediated efflux followed by postefflux events such as bioprecipitation or biological sequestration (1, 7). In this report, the ability of *R. metallidurans* CH34 to resist also selenite is described for the first time. The

physiological and morphological changes resulting from the presence of selenite in the culture medium were studied by using direct chemical assay for selenite, electron microscopy, and electron-dispersive X-ray analysis. The speciation of selenium was determined by X-ray absorption spectroscopy techniques.

## MATERIALS AND METHODS

**Strain and growth media.** *R. metallidurans* CH34 was grown under aerobic conditions at 29°C in the minimal mineral medium described in reference 15. As this medium is buffered with Tris, it is called Tris salt medium (TSM) herein. As previously described (15), TSM was supplemented with the trace element solution SL7 (2) and ferric ammonium citrate. Gluconate was used as a carbon source at a 0.2% final concentration for routine experiments. When high concentrations of cells were required, TSM was supplemented with 1% gluconate. For the determination of the selenite MIC, solid TSM-agar containing increasing amounts of selenite was used. Colonies were counted after 5 days at 29°C.

**Electron microscopy and EDX analysis.** Cells were first fixed at room temperature in 2.5% glutaraldehyde in 0.1 M cacodylate buffer (pH 7.2) for 60 min and then washed three times with the same cacodylate buffer. The cell pellets were fixed for 60 min at 4°C in 1% $OsO_4$ in cacodylate buffer before being dehydrated with ethanol and embedded in Epon. Sections were realized with an ultramicrotome (model S; Leica) equipped with a diamond knife. Uranyl acetate and lead citrate were used as contrast agents. Observations were done with an electron microscope (JEOL 1200EXII) working at 80 kV. Energy-dispersive X-ray (EDX) analysis was performed on the same grids with a scanning transmission electron microscope (JEOL 2000FX) working at 200 kV and equipped with a Princeton Gamma-Tech analysis system.

**X-ray absorption spectroscopy.** Selenium K-edge X-ray absorption experiments were performed on the BM32 beamline at the European Synchrotron Radiation Facility. Reference compounds including hexagonal (i.e., gray) Se for Se(0), $Na_2SeO_3$ for Se(IV), and $Na_2SeO_4$ for Se(VI) were diluted with inert BrN, and the mixture was pressed into 13-mm-diameter pellets. The bacterial material was recorded in both the fresh and freeze-dried states. Freeze-dried bacteria were ground in an agate mortar and pressed into 13-mm-diameter pellets. Fresh bacteria were loaded into a 7-mm-thick liquid sample holder, and the spectrum was recorded immediately. All the spectra were recorded at room temperature in transmission mode. The acquisition time was about 45 min per spectrum. X-ray absorption near-edge structure (XANES) and extended X-ray absorption fine-structure (EXAFS) data extraction and analysis were performed using the WinXAS code (18). Normalized, background-subtracted EXAFS spectra $\chi$, expressed as a function of the electron wave vector $k$, were multiplied by $k^3$ and Fourier transformed using a Bessel window. The structural parameters for the

* Corresponding author. Mailing address: Laboratoire de Chimie et Biochimie des Centres Redox Biologiques, CEA-Grenoble, DBMS/CB-CNRS-Université Joseph Fourier, 38054 Grenoble Cedex 9, France. Phone: 33-(0)4-76-88-91-22. Fax: 33-(0)4-76-88-91-24. E-mail: jcoves@cea.fr.
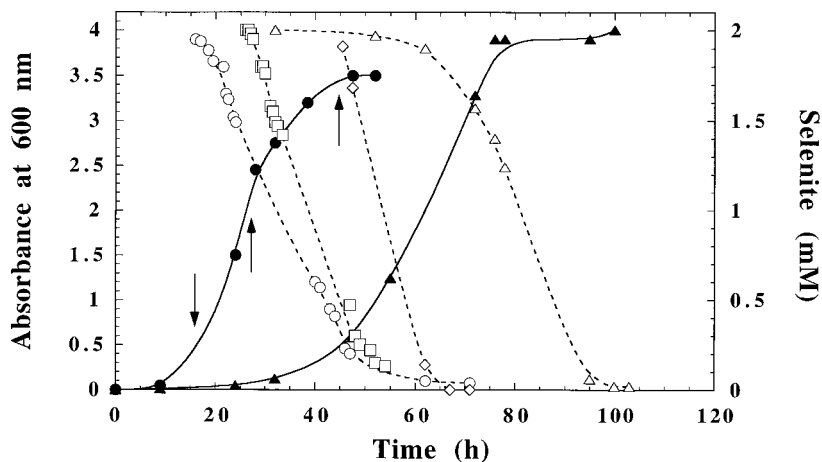
FIG. 1. Time course of growth (filled symbols) and selenite disappearance (open symbols) in *R. metallidurans* CH34. Cells were grown in mineral medium containing 1% gluconate in the absence (●) or in the presence (▲) of 2 mM selenite. Selenite (2 mM) was added at zero time (△) or, for the cultures inoculated in the absence of selenite, at an absorbance at 600 nm of 0.7 (○), 1.5 (□), or 3.2 (◇). Arrows indicate when selenite was added.

first atomic shell around Se (see Fig. 4) were determined by numerical simulation of the first-shell contribution in the real space (in angstroms) and in the reciprocal space (per angstrom) using theoretical FEFF (17) functions calculated from the structure of hexagonal Se (11). The parameters $S_0^2$ (scaling factor) and $\Delta E_0$ (difference in threshold energy between theoretical reference functions and experimental spectra) were determined by simulation of the hexagonal Se spectrum and were fixed for the simulation of the unknown spectrum. Errors, estimated for an increase of the residual $Q$ ($\Sigma\{[k^3\chi(k)_{exp} - k^3\chi(k)_{theo}]/k^3\chi(k)_{exp}\}$) to $2Q$, were 0.01 Å for $R$ and 15% for $N$.

**Selenite content determination.** Selenite concentration was determined by means of the absorbance at 377 nm of a selenium-2,3-diaminonaphthalene complex in cyclohexane as described in reference 12.

## RESULTS

**Resistance of *R. metallidurans* CH34 to selenite stress.** Quantitative selenite susceptibility tests were performed by culture on solid TSM-agar containing increasing concentrations of selenite. The number of colonies was determined after 5 days of growth at 29°C and did not vary during 5 additional days. The MIC, defined as the lowest concentration of inhibitor preventing growth, was found to be about 6 mM selenite under these conditions. During growth in the presence of less than 6 mM selenite, all the colonies turned red, with some delays occurring from one colony to another.

Figure 1 shows a typical growth curve of *R. metallidurans* CH34 in TSM at 29°C. A lag phase of about 15 h was observed before the exponential growth phase. The lag time increased when selenite was added to the culture medium (Fig. 1), and this increase was a function of the selenite concentration (not shown). This behavior was independent of the gluconate concentration. On the other hand, during the exponential phase, bacteria in selenite-complemented media grew at rates comparable to those of bacteria grown in selenite-free media. Furthermore, maximal densities were very similar whether or not selenite was present in the culture medium. In order to know whether this capacity to resist selenite was due to an adaptation to the environmental conditions during the lag phase rather than a mutation, cells grown in the presence of 1 or 2 mM selenite were plated on solid TSM-agar in the absence of selenite. Then the resulting colonies were grown again in the

presence or in the absence of selenite. The duration of the lag phase was still a function of the selenite concentration, as described above. This result showed that *R. metallidurans* CH34 adapted its metabolism to selenite stress during the lag phase and strongly suggests that this adaptation was not the consequence of a mutation.

**The medium can be completely depleted of selenite.** Liquid TSM containing 2 mM selenite was first inoculated with *R. metallidurans* CH34. Then the concentration of selenite in the medium and cell growth were monitored as a function of time. The decrease in selenite concentration started only at the end of the exponential phase ($A_{600} > 3$) and then accelerated during the transition between the exponential phase and the stationary phase. The medium was then completely depleted of selenite during the stationary phase (Fig. 1). In another experiment, 2 mM selenite was added at different times during the exponential phase to cell cultures initiated in the absence of selenite. The decrease in selenite concentration was again measured as a function of time (Fig. 1). In all cases, independently of the cell density at the moment of the addition, introduction of 2 mM selenite had no or only a minor effect on the cell growth rate (not shown) and the totality of the selenite was removed from the medium once the stationary phase was reached. The depletion rate of selenite from the culture medium seems to be related mainly to the cell density. During the first two hours, the concentration of selenite decreased by 0.23, 0.18, or 0.06 mM when 2 mM selenite was added at an absorbance of 3.2, 1.5, or 0.7, respectively. Moreover, when *R. metallidurans* CH34 was grown in the presence of 0.2% gluconate and 2 mM selenite, the stationary phase was reached with an absorbance at 600 nm of about 1 to 1.2 and without a significant evolution of the selenite concentration (not shown). The cell density was not high enough to allow an efficient reduction of the selenite.

Finally, the decrease in selenite concentration was correlated with a reddening of the cell suspension, suggesting an uptake of the oxyanion and its reduction to elemental selenium.
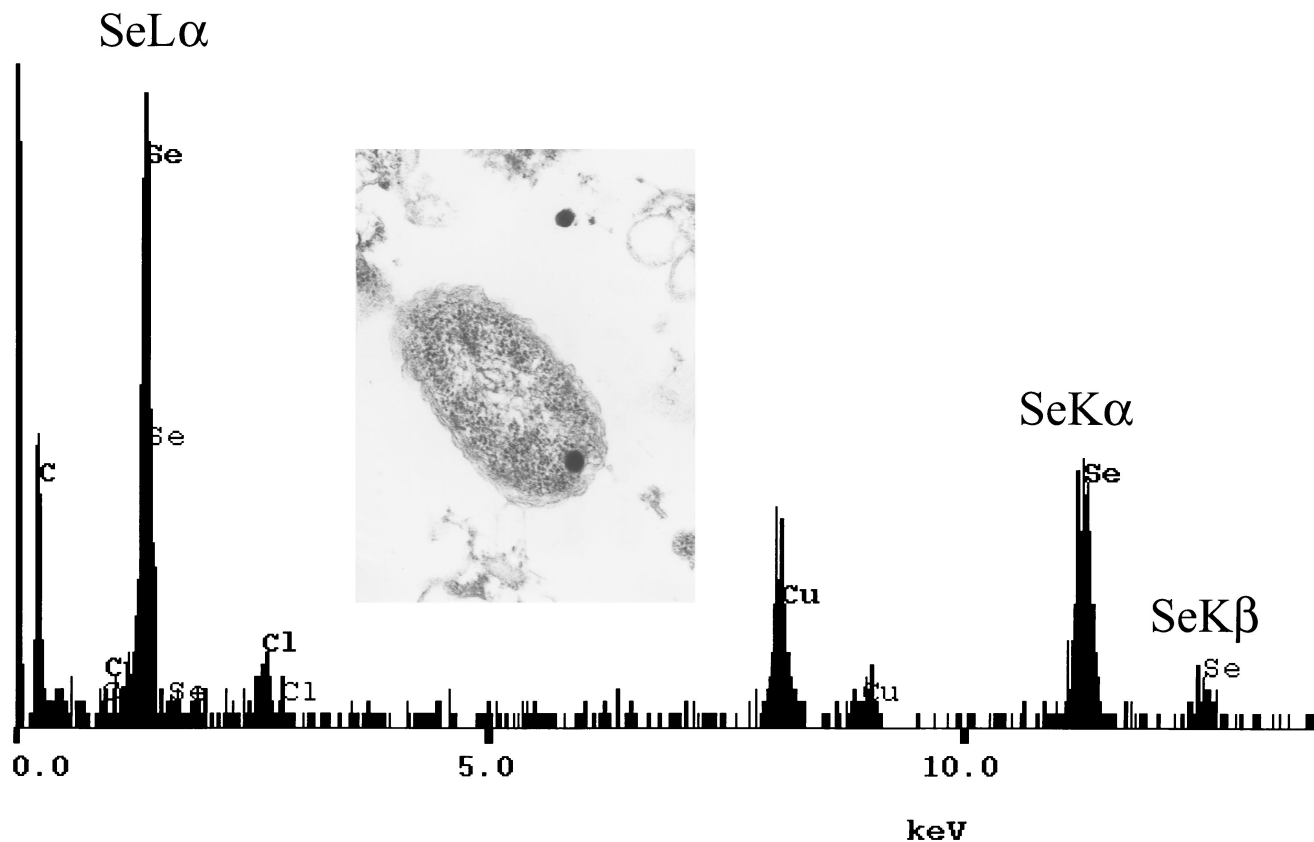
FIG. 2. EDX analysis of the electron-dense body contained in an *R. metallidurans* CH34 cell grown in the presence of 2 mM selenite. The emission lines specific for selenium are identified as SeLα (1.37 keV), SeKα (11.22 keV), and SeKβ (12.49 keV).

**The red color is due to the accumulation of elemental selenium.** Cultures in liquid medium containing 1% gluconate as the carbon source reached an absorbance at 600 nm of 4 to 5 and turned red during the transition between the exponential phase and the stationary phase. When red cultures were centrifuged, the coloration appeared to be associated with the cell pellet and the supernatant was clear and colorless. Washing the cells did not remove the red color.

Electron microscopy allows the detection of electron-dense particles in cells grown in the presence of selenite. Round bodies were found essentially in the cytoplasm (Fig. 2). It was also possible to observe these particles in the periplasm and very rarely in both locations (not shown). In most cases, the dense particles seemed to be associated with or close to a membrane system, but electron-dense granules were also observed without any contact with membranes. In some minor cases, dense deposits were observed in the culture medium, probably coming from dead or damaged cells. However, spoiled cells or cell-like structures lacking internal organization were very rarely observed. Finally and still more scarcely, it was also possible to observe multiple dense bodies, apparently associated with the exterior of the external membrane. The presence of selenium in the electron-dense particles was unambiguously identified by EDX analysis as the specific absorption peaks at 1.37, 11.22, and 12.49 keV were recorded (Fig. 2).

The exact chemical form of selenium in *R. metallidurans*

CH34 was determined by Se K-edge XANES and EXAFS spectroscopies. XANES and EXAFS spectra for the fresh and freeze-dried material were very similar (Fig. 3) and strongly suggested that Se(IV) initially present in the growing culture was transformed into Se(0). However, the radial-structure functions for gray Se taken as a model compound and freeze-dried bacteria were very different (Fig. 4), thus suggesting that the red form was predominant. The structural parameters for the first atomic shell of Se in gray hexagonal Se and in the bacteria were determined by numerical simulation of the Fourier filtered EXAFS spectra. The Se local structure was composed of 2 ± 0.3 Se atoms at 2.37 ± 0.01 Å in hexagonal Se and of 1.8 ± 0.3 Se atoms at 2.34 ± 0.01 Å in *R. metallidurans* CH34. The Se-to-Se distance for the bacteria matches the crystallographic values of red Se (4, 9, 13) and not that of gray Se. Simulations of the bacterial spectrum by a C, O, N, or S shell were completely out of fit, so the presence of organic selenium such as selenium-containing amino acids or organic acids could be ruled out. Thus, EXAFS results allow us to conclude that the metal is present as red Se(0) in the bacteria.

## DISCUSSION

*R. metallidurans* CH34 has been found in the metal-rich sediments of a zinc factory in Belgium and has been demonstrated to prevail in industrial anthropogenic biotopes such as metallurgic wastes (14, 15). It harbors plasmid-borne multiple
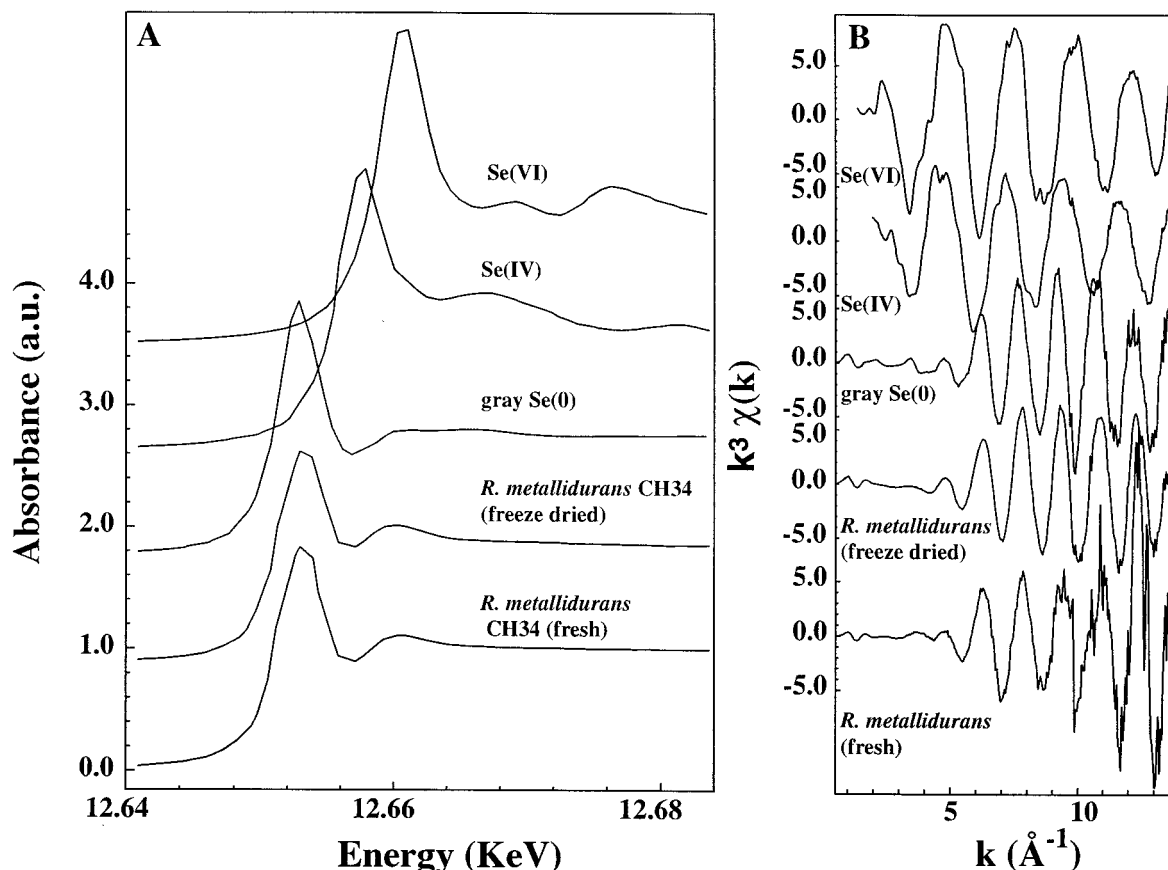
FIG. 3. Se K-edge XANES spectra (A) and Se K-edge EXAFS spectra (B) for selenate [Se(VI)], selenite [Se(IV)], gray selenium [Se(O)], and freeze-dried and fresh bacteria. a.u., arbitrary units.

resistance to heavy metals and oxyanions. This report describes a new capacity of resistance for this strain as it is here demonstrated to resist up to 5 to 6 mM selenite when it is cultured in solid minimal mineral medium. This value must be compared to the MICs determined for other naturally occurring phototrophic and telluric species such as *Rhodobacter sphaeroides*, *Rhodospirillum rubrum*, and *B. subtilis*, which range from about 2 to 5 mM depending on the growth conditions (10, 12, 16). *R. metallidurans* CH34 is thus highly resistant to selenite.

Among the different mechanisms of metal resistance, cation efflux is widely represented (21, 22). However, in the case of selenite, a reduction process seems to be involved. This process leads to accumulation of elemental selenium as electron-dense round bodies within the cells. X-ray absorption spectroscopy is particularly adapted to determine the chemical forms of metals in natural and biological systems without any sample pretreatment (20). Both XANES and EXAFS analyses were previously used to monitor the reduction of Se(IV) into Se(0) by *B. subtilis* (3). In that study, XANES analysis allowed the identification of elemental selenium whereas EXAFS analysis failed to distinguish between the gray and the red forms, as the interatomic distances determined for red and gray Se(0) did not correspond to crystallographic values. Only XANES analysis was used in a very recent study addressing the fate of

selenate and selenite metabolized by *R. sphaeroides* (23). In the present study, EXAFS analysis was used to provide evidence for the accumulation of red selenium in *R. metallidurans* CH34 cells. EXAFS spectra can be simulated using ab initio calculations and allow determination of structural parameters such as the nature and the number of neighboring atoms around Se and the interatomic distances. The values deduced from the experiment with bacteria and from the calculations fit perfectly those determined for the different crystallographic forms of red selenium (4, 9, 13).

Most of the time, only one electron-dense particle of selenium per cell was visible. The location of elemental selenium was mostly in the cytoplasm, either close or not close to the inner membrane system. In some cases, an electron-dense particle was found in the periplasm. As it is difficult to imagine that such large particles can be transported across the inner membrane and as we never observed a vesicular mechanism of excretion, we suggest that selenite can be reduced either in the periplasm or in the cytoplasm and that elemental selenium accumulates where it is produced. As selenium is in a redox state of (+IV) in selenite and of (−II) in biomolecules or (0) in elemental selenium, the question of the nature and of the specificity of the reduction system arises. The chemical basis for the reduction of selenite to selenium is largely unknown and is now under investigation.
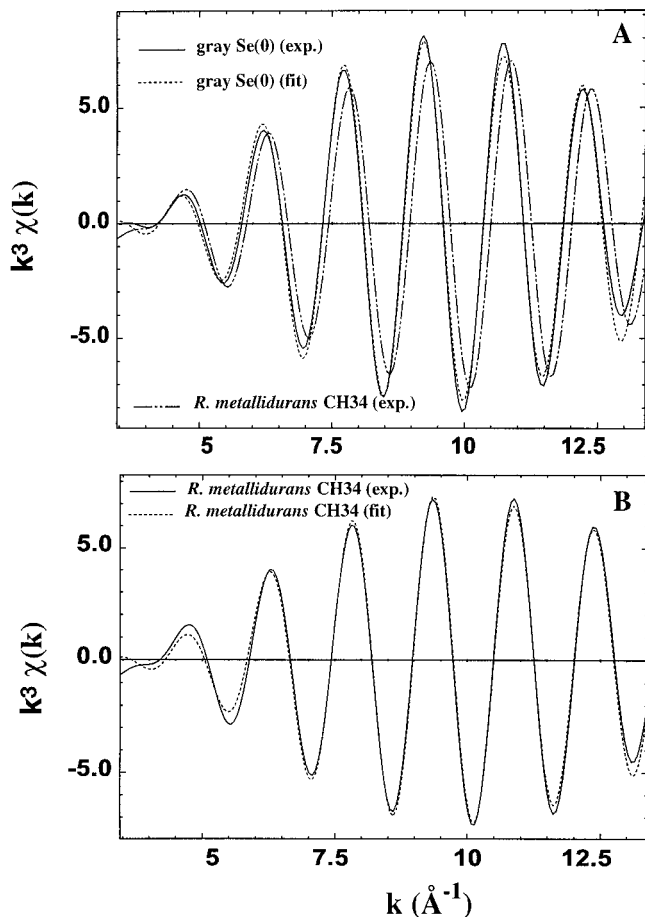
FIG. 4. Numerical simulation of the Fourier filtered contribution of the first Se atomic shell for gray Se (A) and freeze-dried bacteria (B), which allows the determinations of the Se-to-Se interatomic distance $R$ (in angstroms), of the coordination number $N$, and of the Debye-Waller factor $\sigma^2$ (in square angstroms), which accounts for the thermal and static disorder. $R$, $N$, and $\sigma^2$ values obtained are 2.37 Å, 2 Se atoms, and 0.0040 Å$^2$ for hexagonal Se and 2.34 Å, 1.8 Se atoms, and 0.0040 Å$^2$ for *R. metallidurans* CH34. exp., experimental.

*R. metallidurans* CH34 has already been used, at least at an experimental level, in bioremediation processes leading to removal of heavy metals from soil or liquid waste (6, 8, 14). As a result of its insolubility, elemental selenium becomes essentially not bioavailable and nontoxic. Thus, the finding that *R. metallidurans* CH34 can also resist selenite by reducing it to and accumulating it as selenium granules makes this microorganism also a candidate for the restoration of selenite-polluted biotopes.

### ACKNOWLEDGMENTS

## REFERENCES

1. **Anton, A., C. Grosse, J. Reissmann, T. Pribyl, and D. H. Nies.** 1999. CzcD is a heavy metal ion transporter involved in regulation of heavy metal resistance in *Ralstonia* sp. strain CH34. J. Bacteriol. **181:**6876–6881.
2. **Biebl, H., and N. Pfennig.** 1981. Isolation of members of the family Rhodospirillaceae, p. 267–273. *In* M. P. Starr, J. Stolp, H. G. Trüper, A. Balows, and H. G. Schlegel (ed.), The prokaryotes, a handbook on habitats, isolation and identification of bacteria, vol. A. Springer-Verlag, Berlin, Germany.
3. **Buchanan, B. B., J. J. Bucher, D. E. Carlson, N. M. Edelstein, E. A. Hudson, N. Kaltsoyannis, T. Leighton, W. Lukens, D. K. Shuh, H. Nitsche, T. Reich, K. Roberts, P. Torretto, J. Woicik, W.-S. Yang, A. Yee, and B. C. Yee.** 1995. A XANES and EXAFS investigation of the speciation of selenite following bacterial metabolization. Inorg. Chem. **34:**1617–1619.
4. **Cherin, P., and P. Hunger.** 1972. Refinement of crystal structure of alpha monoclinic Se. Acta Crystallogr. **B28:**313–317.
5. **Conde, J. E., and M. Sanz Alaejos.** 1997. Selenium concentrations in natural and environmental waters. Chem. Rev. **97:**1979–2003.
6. **Diels, L., M. De Smet, L. Hooyberghs, and P. Corbisier.** 1999. Heavy metals bioremediation of soil. Mol. Biotechnol. **12:**149–158.
7. **Diels, L., Q. Dong, D. van der Lelie, W. Baeyens, and M. Mergeay.** 1995. The czc operon of *Alcaligenes eutrophus* CH34: from resistance mechanism to the removal of heavy metals. J. Ind. Microbiol. **14:**142–153.
8. **Diels, L., S. van Roy, K. Somers, I. Willems, W. Doyen, M. Mergeay, D. Springael, and R. Leysen.** 1995. The use of bacteria immobilized in tubular membrane reactors for heavy metal recovery and degradation of chlorinated aromatics. J. Membr. Sci. **100:**249–258.
9. **Foss, O., and V. Janickis.** 1980. Crystal structure of the gamma-monoclinic selenium. J. Chem. Soc. Dalton Trans. **4:**624–627.
10. **Garbisu, C., D. Carlson, M. Adamkiewicz, B. C. Yee, J. H. Wong, E. Resto, T. Leighton, and B. B. Buchanan.** 1999. Morphological and biochemical responses of Bacillus subtilis to selenite stress. Biofactors **10:**311–319.
11. **Keller, R., W. B. Holzapfel, and H. Schulz.** 1977. Effect of the pressure on the atom position in Se and Te. Phys. Rev. **B16:**4404–4412.
12. **Kessi, J., M. Ramuz, E. Wehrli, M. Spycher, and R. Bachofen.** 1999. Reduction of selenite and detoxification of elemental selenium by the phototrophic bacterium *Rhodospirillum rubrum*. Appl. Environ. Microbiol. **65:**4734–4740.
13. **Marsh, R. E., L. Pauling, and J. D. McCullough.** 1952. The crystal structure of beta selenium. Acta Crystallogr. **5:**236–246.
14. **Mergeay, M.** 2000. Bacteria adapted to industrial biotopes: metal-resistant *Ralstonia*, p. 403–414. *In* G. Storz and R. Hengge-Aronis (ed.), Bacterial stress responses. American Society for Microbiology, Washington, D.C.
15. **Mergeay, M., D. Nies, H. G. Schlegel, J. Gerits, P. Charles, and F. Van Gijsegem.** 1985. *Alcaligenes eutrophus* CH34 is a facultative chemolithotroph with plasmid-bound resistance to heavy metals. J. Bacteriol. **162:**328–334.
16. **Moore, M. D., and S. Kaplan.** 1992. Identification of intrinsic high-level resistance to rare-earth oxides and oxianions in members of the class *Proteobacteria*: characterization of tellurite, selenite, and rhodium sesquioxide reduction in *Rhodobacter sphaeroides*. J. Bacteriol. **174:**1505–1514.
17. **Rehr, J. J., J. Mustre de Leon, S. I. Zabinski, and R. C. Albers.** 1991. Theoretical X-ray absorption fine structure standards. J. Am. Chem. Soc. **113:**5135–5145.
18. **Ressler, T.** 1997. WinXAS: a new software package not only for the analysis of energy-dispersive XAS data. J. Phys. Colloq. **2:**269–270.
19. **Saiki, M. K., and T. P. Lowe.** 1987. Selenium in aquatic organisms from subsurface agricultural drainage water, San Joaquin Valley, California. Arch. Environ. Contam. Toxicol. **16:**657–670.
20. **Schulze, D. G., and P. M. Bertsch.** 1995. Synchrotron X-ray techniques in soil, plant, and environmental research. Adv. Agron. **55:**1–66.
21. **Tibazarwa, C., S. Wuertz, M. Mergeay, L. Wyns, and D. van der Lelie.** 2000. Regulation of the *cnr* cobalt and nickel resistance determinant of *Ralstonia eutropha* (*Alcaligenes eutrophus*) CH34. J. Bacteriol. **182:**1399–1409.
22. **van der Lelie, D., T. Schwuchow, U. Schwidetzky, S. Wuertz, W. Baeyens, M. Mergeay, and D. H. Nies.** 1997. Two-component regulatory system involved in transcriptional control of heavy-metal homoeostasis in *Alcaligenes eutrophus*. Mol. Microbiol. **23:**493–503.
23. **Van Fleet-Stalder, V., T. G. Chasteen, I. J. Pickering, G. N. George, and R. C. Prince.** 2000. Fate of selenate and selenite metabolized by *Rhodobacter sphaeroides*. Appl. Environ. Microbiol. **66:**4849–4853.